iScience

CellPress
OPEN ACCESS

Article

Insights into Manipulating Postprandial Energy Expenditure to Manage Weight Gain in Polycystic Ovary Syndrome

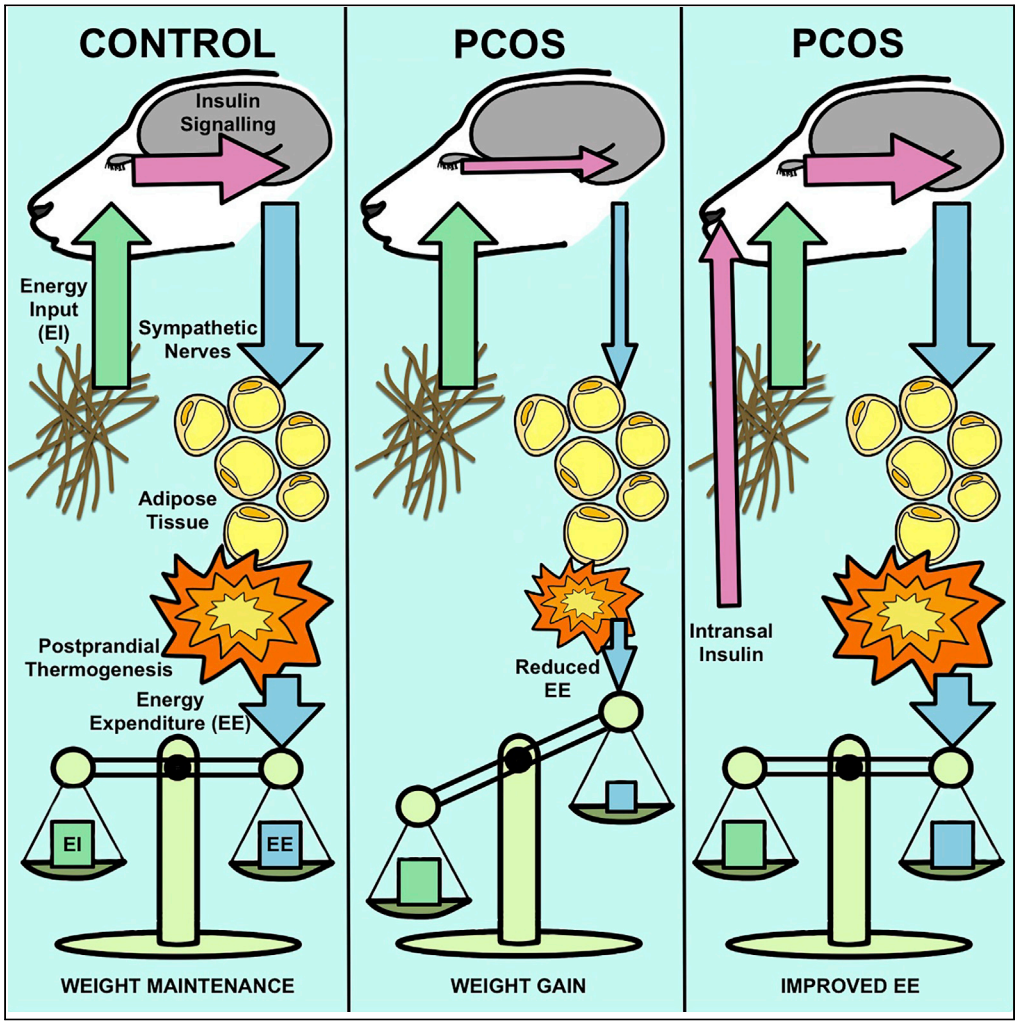

Katarzyna Siemienowicz, Michael T. Rae, Fiona Howells, Chloe Anderson, Linda M. Nicol, Stephen Franks, William C. Duncan

w.c.duncan@ed.ac.uk

HIGHLIGHTS

Obesity can be prenatally programmed by androgens in an ovine model of PCOS

This model has the same deficit in postprandial energy expenditure as women with PCOS

Reduced adipose tissue thermogenesis links to lower central insulin signaling

Therapeutic intranasal insulin raises postprandial energy expenditure in PCOS sheep

Siemienowicz et al., iScience *23*, 101164
June 26, 2020 © 2020 The Author(s).
https://doi.org/10.1016/j.isci.2020.101164

iScience

CellPress
OPEN ACCESS

Article

Insights into Manipulating Postprandial Energy Expenditure to Manage Weight Gain in Polycystic Ovary Syndrome

Katarzyna Siemienowicz,[1,2] Michael T. Rae,[2] Fiona Howells,[1] Chloe Anderson,[1] Linda M. Nicol,[1] Stephen Franks,[3] and William C. Duncan[1,4,*]

SUMMARY

Women with polycystic ovary syndrome (PCOS) are more likely to be obese and have difficulty in losing weight. They demonstrate an obesity-independent deficit in adaptive energy expenditure. We used a clinically realistic preclinical model to investigate the molecular basis for the reduced postprandial thermogenesis (PPT) and develop a therapeutic strategy to normalize this deficit. Sheep exposed to increased androgens before birth develop the clinical features of PCOS. In adulthood they develop obesity and demonstrate an obesity-independent reduction in PPT. This is associated with reduced adipose tissue uncoupling protein expression and adipose tissue noradrenaline concentrations. These sheep are insulin resistant with reduced insulin signaling in the brain. Increasing brain insulin concentrations using intranasal insulin administration increased PPT in PCOS sheep without any effects on blood glucose concentrations. Intranasal insulin administration with food is a potential novel strategy to improve adaptive energy expenditure and normalize the responses to weight loss strategies in women with PCOS.

INTRODUCTION

Polycystic ovary syndrome (PCOS) is common, affecting 7%–8% of women of reproductive age, and its incidence is increasing (Fauser et al., 2012). Metabolic dysfunction in PCOS causes lifelong disease and negatively affects the health and well-being of women, their economic productivity, and health service resources (Jason, 2011). Up to 80% of women with PCOS are overweight or obese (body mass index [BMI] >25 kg/m^2), and in Australia and the United States the prevalence of obesity (BMI >30 kg/m^2) in women with PCOS is as high as 61%–76% (Fauser et al., 2012). Women with PCOS rate obesity as a major concern (Sill et al., 2001), and increased BMI in PCOS is associated with markedly reduced quality-of-life scores (Ching et al., 2007). In addition, women with PCOS are more likely to develop glucose intolerance and diabetes (Palomba et al., 2009). By 30 years of age, 5%–10% of women with PCOS already have type 2 diabetes, 30%–40% have impaired glucose tolerance, and up to 40% will develop gestational diabetes during pregnancy (Legro et al., 2005). As the metabolic consequences of PCOS are markedly exacerbated by obesity, and women with PCOS are more likely to be obese, understanding and targeting obesity in PCOS is critically important. The European Society of Human Reproduction and Embryology (ESHRE)/American Society for Reproductive Medicine (ASRM) consensus on health aspects of PCOS highlighted that "Mechanistic studies are necessary to understand the evolution of obesity and PCOS" (Fauser et al., 2012).

Obesity can be due to increased energy intake, reduced energy expenditure (EE), or their combinations. Approximately 65% of energy is expended in maintaining physiological function and 20%–25% by physical activity. Thus, increasing physical activity, without an equivalent increase in energy intake, promotes weight loss. The remaining EE is linked to adaptive thermogenesis. Between 10% and 15% of energy is expended after eating in response to dietary intake (Tseng et al., 2010). We have assessed EE after feeding in women with PCOS using continuous indirect calorimetry. These women show an obesity-independent reduction in peak postprandial thermogenesis (PPT) to 73.2% ± 6.9% of weight-matched controls (Robinson et al., 1992). This suggests that the high prevalence of obesity in women with PCOS may be related to altered adaptive thermogenesis that is not a consequence of obesity.

[1]MRC Centre for Reproductive Health, Queen's Medical Research Institute, The University of Edinburgh, Edinburgh EH16 4TJ, UK

[2]School of Applied Sciences, Edinburgh Napier University, Edinburgh EH11 4BN, UK

[3]Institute of Reproductive and Developmental Biology, Imperial College, London W12 0HS, UK

[4]Lead contact

*Correspondence: w.c.duncan@ed.ac.uk

https://doi.org/10.1016/j.isci.2020.101164

This is an open access article under the CC BY-NC-ND license (http://creativecommons.org/licenses/by-nc-nd/4.0/).

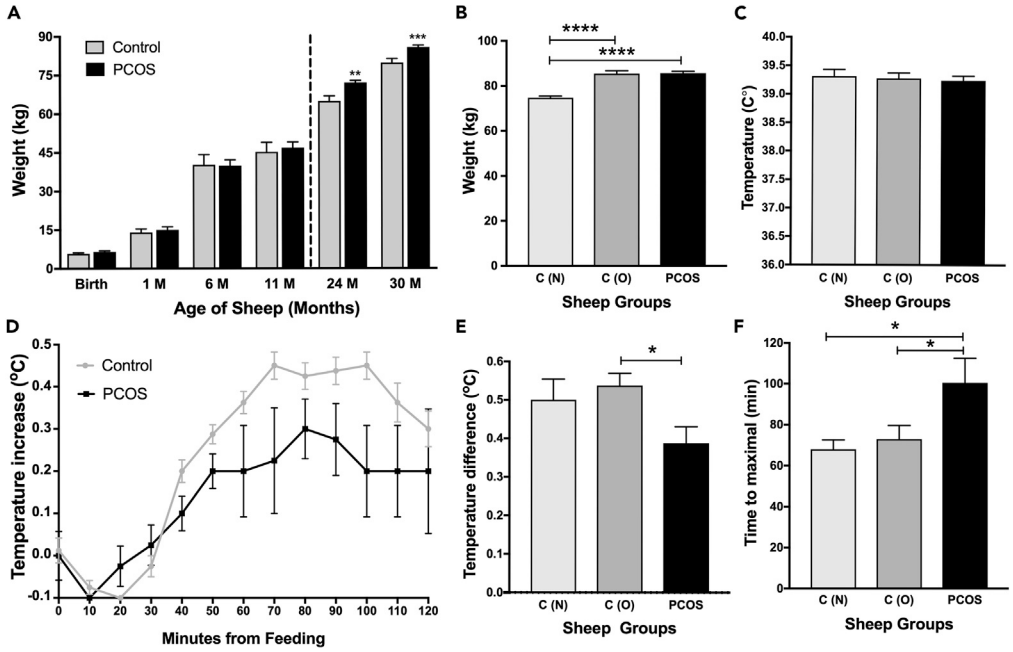

Figure 1. Postprandial Thermogenesis and Weight

(A) Weight of C-sheep (n = 11) and PCOS-sheep (n = 4) from birth to 30 months. Adulthood is indicated by the dotted line.
(B) Two subsets of C-sheep showing the obese (O) (n = 4) and normal (N) (n = 4) controls and the PCOS-sheep (n = 4).
(C) The basal body temperature in the normal (N) C-sheep, the obese (O) C-sheep, and the PCOS-sheep.
(D) The temperature increase after feeding as a function of time in PCOS-sheep and C-sheep at 30 months of age.
(E) The maximal minus the minimum temperature after feeding in the (N) C-sheep, the (O) C-sheep, and the PCOS-sheep.
(F) The time to maximum temperature in the (N) C-sheep, the (O) C-sheep, and the PCOS-sheep. Data are represented as mean ± SEM. *p < 0.05, **p < 0.01, ***p < 0.005, ****p < 0.001.

Adult Scottish Greyface ewes weigh up to 85 kg and are ideally suited to longitudinal preclinical studies involving serial sampling and multiple tissue analysis. The female offspring of women (Barnes et al., 1994), non-human primates (Abbott et al., 2013), and sheep (Padmanabhan and Veiga-Lopez, 2013) exposed to increased androgens during mid-pregnancy manifest ovarian, hormonal, and metabolic phenotypes reminiscent of PCOS. We have used the gestational androgenization ovine model to provide insights into the molecular pathophysiology of PCOS and its antecedents (Ramaswamy et al., 2016) and also to examine therapeutic paradigms (Connolly et al., 2014). After maternal gestational androgen exposure, female offspring develop polycystic ovaries, thecal hyperandrogenism, progressive insulin resistance (IR), and fatty liver in adulthood (Ramaswamy et al., 2016; Connolly et al., 2014; Hogg et al., 2011, 2012; Rae et al., 2013). Using the protocol described in this article 100% control sheep regularly ovulated in the second breeding season, at around 2 years of age, whereas only 25% PCOS sheep showed any evidence of ovulation.

We hypothesized that the ovine model of PCOS could be used to dissect the pathophysiology of impaired PPT in women and inform and test novel treatment paradigms. Herein we show that sheep prenatally programmed to have PCOS have increased weight in adulthood and this is associated with an obesity-independent deficit in PPT, of the same magnitude as that seen in women with PCOS, which is correlated with IR. Using this clinically realistic model we investigated EE in adipose tissue and its sympathetic stimulation as well as insulin signaling in the brain. We then investigated whether increasing insulin signaling in the brain using an intranasal insulin (INI) aerosol spray could safely normalize adaptive EE after feeding.

RESULTS

Increased Body Weight in the Ovine PCOS Model

Female offspring of sheep exposed to increased androgens during pregnancy (PCOS-sheep) show no difference in birth weight or body weight during the first year of life, through puberty and adolescence

(Figure 1A). However, in adulthood, at 2 years of age, they have increased body weight when compared with control animals (C-sheep) (PCOS-sheep: 72.0 ± 0.91 kg; C-sheep: 64.9 ± 1.98 kg; $p = 0.006$). This increase in body weight is maintained until the end of the experiment at 30 months of age (PCOS-sheep: 85.75 ± 0.75 kg; C-sheep 79.73 ± 1.58 kg; $p = 0.004$; Figure 1A). PCOS-sheep are prenatally programmed to develop increased body weight in adult life.

Deficit in Postprandial Thermogenesis

We selected the four heaviest C-sheep (85.5 ± 1.25 kg), whose weight was not different from that of the PCOS-sheep ($p = 0.98$), and the four lightest C-sheep (74.75 ± 0.75 kg), which were significantly lighter than the heaviest C-sheep ($p < 0.0001$) and the PCOS-sheep (Figure 1B, $p < 0.0001$), for further detailed study. PPT was examined by direct temperature sensing from the interscapular adipose tissue using datalogger-implanted thermometers. There were no differences in basal body temperature between the C-sheep and PCOS-sheep (Figure 1C). After feeding, all sheep had robust and predictable PPT manifest by a temperature increase. PCOS-sheep had a significant reduction in PPT ($p < 0.05$; Figure 1D) when compared with C-sheep. This was the same regardless of the weight of the C-sheep. The reduction of EE after feeding in the PCOS-sheep was 74.7% ± 8.2% of that of controls and 72.1% ± 7.9% of weight-matched controls (Figure 1E). Along with reduction in the temperature increase, the PCOS-sheep took longer to reach this maximal temperature ($p < 0.05$; Figure 1F). PCOS-sheep are prenatally programmed to have reduced PPT.

Association with Insulin Resistance

At 2 years of age the PCOS-sheep were hyperinsulinemic. They showed no differences in glucose dynamics during an intravenous glucose tolerance test (GTT) (Figure 2A), but they had significantly increased area under the curve insulin concentrations ($p < 0.05$; Figures 2B and S1). At that stage the fasting insulin concentrations were not different from controls ($p = 0.298$; Figure 2C). However, at 30 months of age fasting insulin was increased in PCOS-sheep ($p < 0.05$; Figures 2D and S1). They showed evidence of IR in the fasting state with reduced basal glucose to insulin ratio ($p < 0.05$; Figures 2E and S1). Fasting insulin concentrations showed a negative correlation with the temperature difference during PPT ($R = -0.56$, $p < 0.05$; Figure 2F) and a positive correlation with the time to maximal temperature ($R = 0.56$, $p < 0.05$; Figure 2G). The reduction in PPT correlates with the degree of IR.

Molecular Analysis of Muscle and Fat Depots

We examined the expression of genes linked to thermogenesis and calcium cycling in skeletal muscle. There were no differences in their transcript abundance in the muscle of PCOS-sheep when compared with C-sheep (Figure 3A). We next examined the expression of the transcripts of thermogenic uncoupling proteins in four different adipose tissue sites (Figure 3B). *UCP1* was reduced in both subcutaneous (neck and groin; $p < 0.05$) and visceral ($p < 0.01$) adipose depots (Figures 3C and S1). In addition, *UCP2* ($p < 0.05$) and *UCP3* ($p < 0.05$) were reduced in the subcutaneous back fat (Figures 3D, 3E, and S1). After checking antibody specificity for sheep tissue (Figure S1), immunohistochemistry was carried out for UCP1 and UCP3 in the sites with the biggest differential expression. UCP1 protein could be consistently identified in subcutaneous (groin) fat in C-sheep (Figure 3F), but it was largely absent from PCOS-sheep (Figure 3G). Its expression correlated with the temperature increase after eating ($R = 0.66$, $p < 0.05$; Figure 3H). Similarly, UCP3 protein was clearly seen in the subcutaneous (back) adipose tissue in C-sheep (Figure 3I) and less so in the PCOS-sheep (Figure 3J). Its expression correlated with the thermogenesis response ($R = 0.72$, $p < 0.01$; Figure 3K). The reduction in PPT is associated with reduced UCP expression in adipose tissue.

Reduction in Adipose Tissue Sympathetic Signaling

As adipose tissue UCP expression is primarily regulated by sympathetic innervation we measured the transcript abundance for β-adrenergic receptors in the fat depots (Figure 4A). As there was no difference in receptor expression we measured the content of noradrenaline (NA) in the fat depots. There was a reduction in NA concentrations in subcutaneous (neck and groin) and visceral adipose tissue (Figure 4B). In addition, the mean NA concentrations in all fat depots were significantly lower in PCOS-sheep than control sheep ($p < 0.05$; Figure 4C). The adipose tissue NA concentration correlated with PPT ($R = 0.58$, $p < 0.05$; Figure 4D) and was inversely correlated with body weight ($R = -0.59$; $p < 0.05$; Figure 4E). There is a reduction in the sympathetic drive in the fat depots of PCOS-sheep.

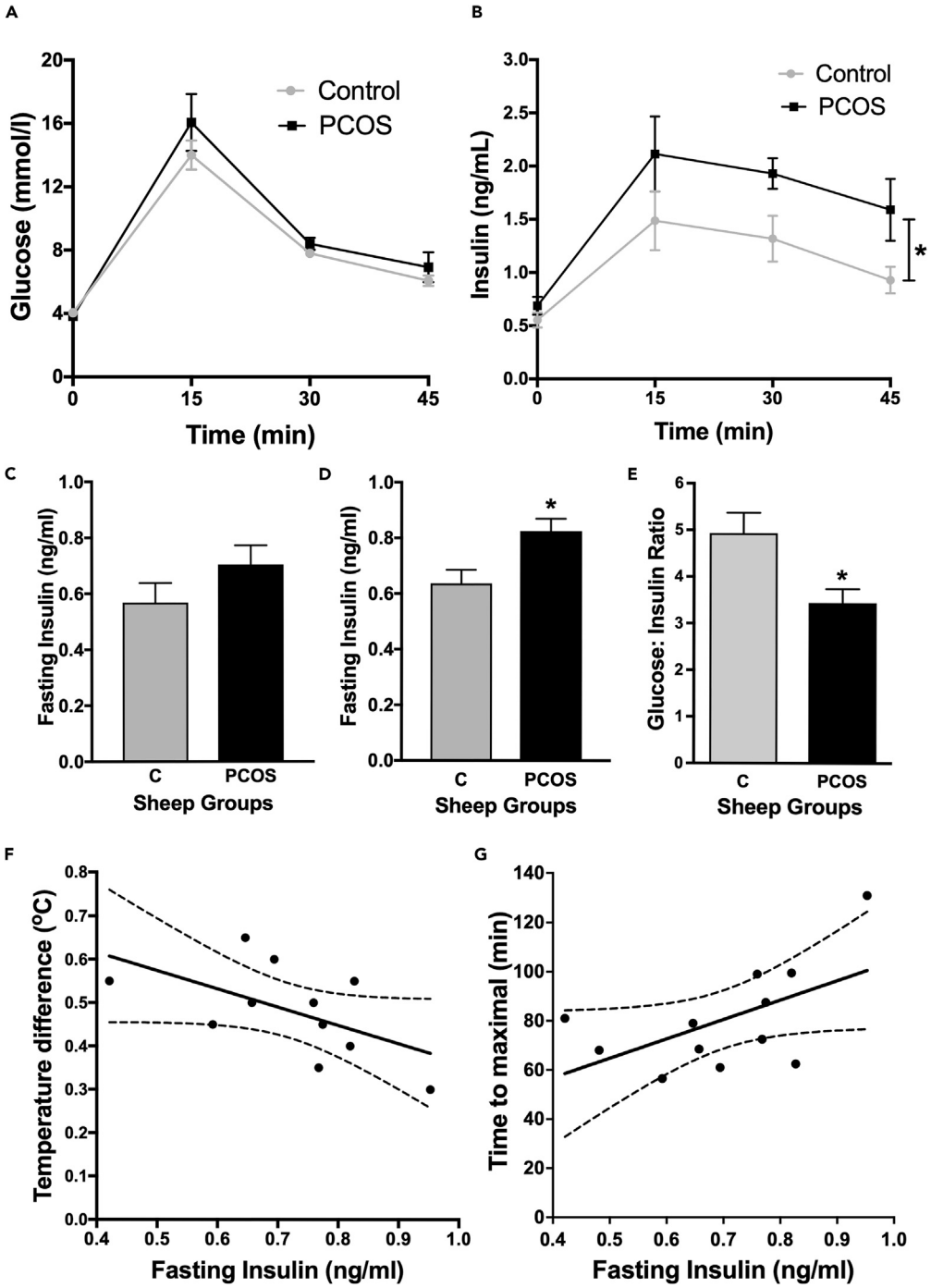

Figure 2. Insulin Resistance

(A and B) (A) Plasma glucose and (B) insulin in the 45 min after an IV GTT in C-sheep and PCOS-sheep at 24 months of age.
(C and D) (C) Fasting insulin concentrations at 24 months and (D) 30 months in C-sheep and PCOS-sheep.
(E) Fasting glucose to insulin ratio in C-sheep and PCOS-sheep at 30 months of age.
(F) Correlation between postprandial temperature difference and fasting insulin concentrations ($p < 0.05$).
(G) Correlation between fasting insulin concentrations and time to maximal postprandial temperature ($p < 0.05$). Data are represented as mean ± SEM. *$p < 0.05$.

A

Relative gene expression in skeletal muscle			
Gene	Control-Sheep	PCOS-Sheep	Significance
RYR1	1.02 ±0.07	0.83 ±0.17	NS
ATP2A1	1.01 ±0.05	0.93 ±0.15	NS
ATP2A2	1.08 ±0.13	0.93 ±0.10	NS
UCP1	1.28 ±0.31	1.34 ±0.26	NS
UCP2	1.09 ±0.13	1.31 ±0.51	NS
UCP3	1.04 ±0.09	1.43 ±0.20	NS

B

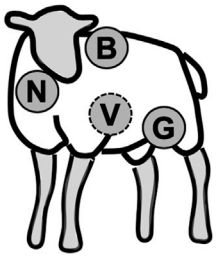

C

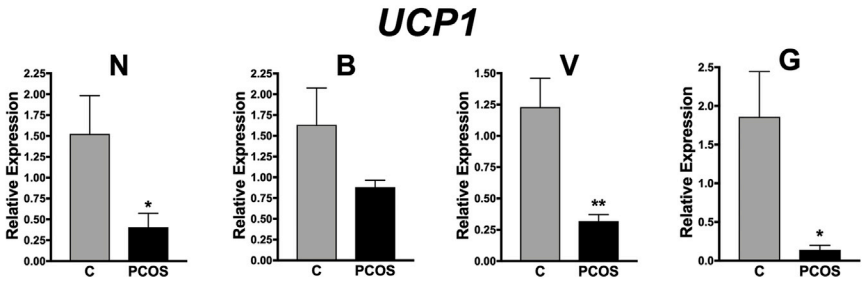

D

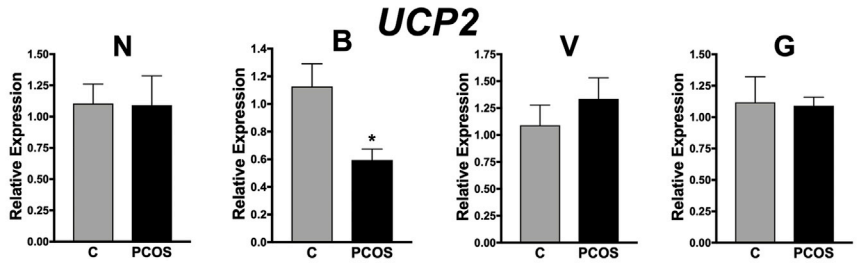

E

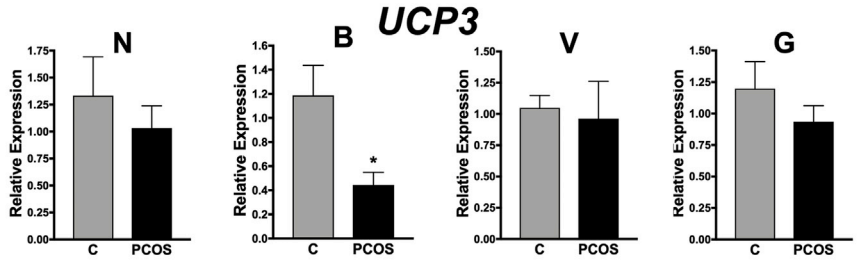

F G H

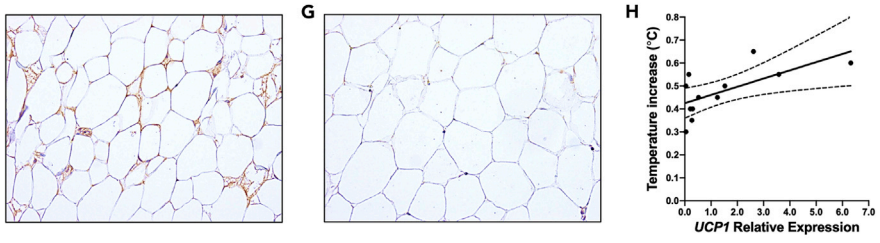

I J K

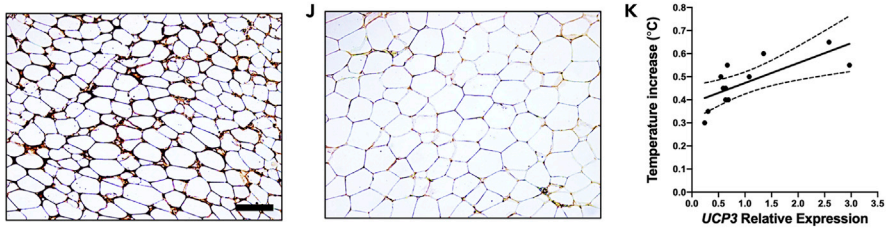

Figure 3. Expression of UCPs

(A) Relative mean gene expression ± SEM measured by RT-PCR in skeletal muscle for uncoupling proteins and genes involved in futile calcium cycling.

(B–J) (B) Diagram highlighting the adipose tissue depots studied: the neck (N) fat, inter-scapular back (B) fat, visceral (V) fat, and subcutaneous groin (G) fat. Relative expression of (C) UCP1, (D) UCP2, and (E) UCP3 in the four adipose tissue depots. Immunohistochemistry for UCP1 (brown) in G fat from (F) C-sheep and (G) PCOS-sheep. (H) Correlation between UCP1 expression in G fat and postprandial temperature increase ($p < 0.05$). Immunohistochemistry for UCP3 (brown) in B fat from (I) C-sheep and (J) PCOS-sheep.

(K) Correlation between UCP3 expression in B fat and postprandial temperature increase ($p < 0.05$). All immunochemistry taken at the same magnification. Scale bar, 100 μm. NS is not significant. Data are represented as mean ± SEM. *$p < 0.05$, **$p < 0.01$).

Central Insulin Signaling in the Ovine PCOS Model

As brain insulin action can regulate sympathetic drive to adipose tissue primarily through hypothalamic action, and IR correlated to reduced PPT, we assessed central insulin signaling in C-sheep and PCOS-sheep. Insulin signaling, assessed by pERK immunohistochemistry, was evident in cells within the hypothalamus (Figure 5A), whereas quantification of the degree of signaling using western blotting in this tissue that has marked functional regional differences was challenging. We therefore examined a consistent region of the frontal cortex. There were no differences in the expression of the key elements of the insulin signaling pathway (Figures 5B–5D). However, there was a difference in insulin signaling (Figure 5E). The reduction in the expression of pAKT almost reached significance ($p = 0.057$; Figure 5F) in PCOS-sheep, whereas cerebral pERK was consistently reduced in PCOS-sheep ($p < 0.05$; Figure 5G). There is evidence for decreased insulin signaling in the brain of PCOS-sheep.

The Effect of Intranasal Insulin of Postprandial Thermogenesis

To test whether raising intracerebral insulin could improve PPT in PCOS-sheep, we developed another cohort of PCOS sheep. The insulin response to an intravenous GTT increased in adolescence at 11 months of age and further increased in adulthood (Figure 6A). At 20 months of age the insulin concentrations (Figure 6B) and basal glucose:insulin ratio (Figure 6C) were outwith age-matched historical controls, suggesting IR. Administration of 10 IU insulin intranasally showed no change in blood glucose concentration over the next hour in one test animal (Figure 6D). In the cohort of PCOS-sheep INI showed no effects on blood glucose over 10 min in the absence (Figure 6E) or presence of food (Figure 6F). Interestingly there was no increase in serum insulin after INI in the absence of food (Figure 6G), but when given with food there was an increase in serum insulin concentrations ($p < 0.05$; Figure 6H), suggesting an endogenous response to food. INI significantly increased the PPT response in PCOS-sheep ($p < 0.05$; Figure 6I). In addition, there was a small effect on PPT with insulin ($p < 0.05$; Figure 6I) in the absence of feeding. Therapeutically increasing cerebral insulin increases PPT in PCOS-sheep.

DISCUSSION

Manipulation of the hormonal environment *in utero* by increasing maternal androgen concentrations has important effects on the female offspring. In adulthood they have increased body weight when compared with control female offspring. As these sheep were genetically outbred, randomly allocated to treatment, and share the same paternal genetic component, this increased weight is environmental rather than genetic. The postnatal sheep share the same postnatal environment suggesting that they are prenatally programmed to become overweight in adult life. This is another example of the far-reaching consequences of endocrine disruption *in utero* and the lifelong importance of the prenatal environment (Gore et al., 2015).

There are numerous examples of developmental programming of adult metabolic dysfunction and a very clear link to fetal undernutrition, lower birthweight, catch-up growth, and ultimate obesity (Ravelli et al., 1976; Hales and Barker, 1992; Isganaitis, 2019). In this case the birthweight was normal as was weight gain until adolescence as increased weight was manifest in early adulthood. However, in similar ovine models of PCOS using testosterone administration from D30 gestation there is some evidence of growth restriction and masculinization of external genitalia at birth (Padmanabhan and Veiga-Lopez, 2013). We have shown that growth restriction is not seen when testosterone is given after the male programming window at D60 gestation. The PCOS-sheep are prenatally programmed to become obese in later life. Obesity in early adulthood is common in women with PCOS (Fauser et al., 2012; Ollila et al., 2016) and like the PCOS-sheep women with PCOS do not show consistent evidence of prenatal undernutrition

A

Relative gene expression in fat depots			
Site	Control-Sheep	PCOS-Sheep	Significance
ADRB1			
N	1.05 ±0.09	1.35 ±0.31	NS
B	1.22 ±0.21	1.57 ±0.33	NS
V	1.06 ±0.12	1.29 ±0.15	NS
G	1.16 ±0.21	1.13 ±0.21	NS
ADRB2			
N	1.09 ±0.14	1.33 ±0.27	NS
B	1.19 ±0.27	1.10 ±0.21	NS
V	1.09 ±0.16	1.41 ±0.08	NS
G	1.11 ±0.20	1.19 ±0.21	NS
ADRB3			
N	1.52 ±0.39	1.03 ±0.41	NS
B	1.37 ±0.53	2.66 ±0.95	NS
V	1.37 ±0.38	1.52 ±0.89	NS
G	ND	ND	-

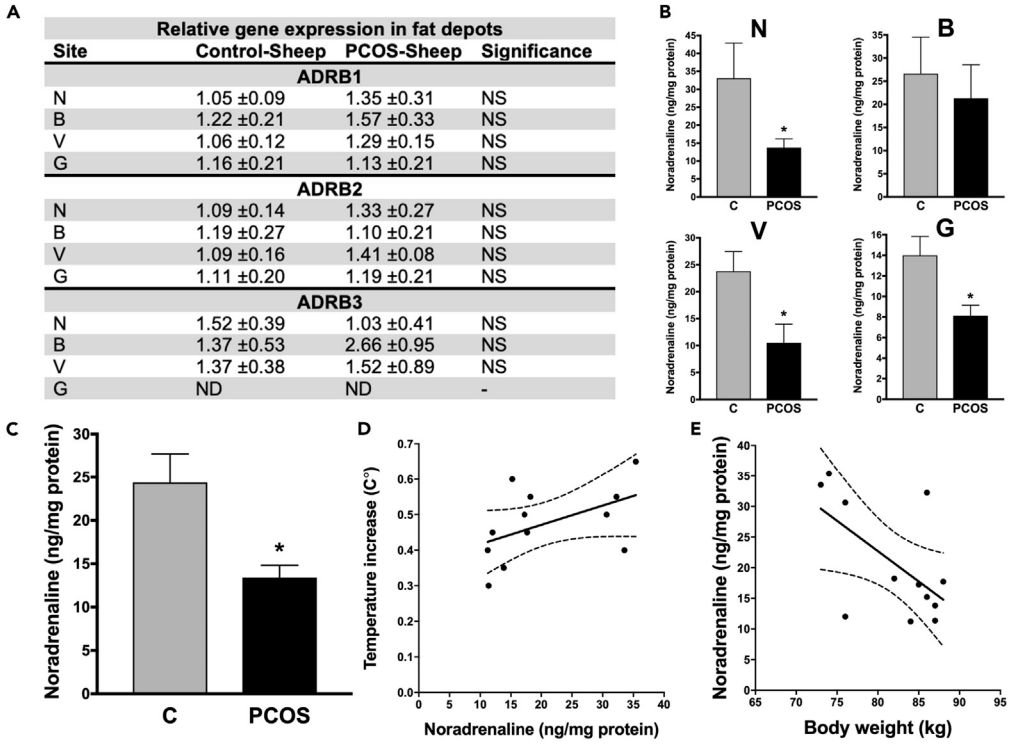

Figure 4. Sympathetic Activity

(A) Relative mean gene expression ± SEM for β-adrenergic receptors, measured by RT-PCR, in the neck (N), interscapular back (B), visceral (V), and subcutaneous groin (G) adipose tissue depots in C-sheep and PCOS-sheep.

(B) NA concentrations in the four adipose tissue depots in C-sheep and PCOS-sheep.

(C–E) (C) Four-site average NA concentrations in adipose tissue in C-sheep and PCOS-sheep. Correlation of adipose tissue NA concentrations and (D) postprandial temperature increase ($p < 0.05$) and (E) body weight at 30 months of age ($p < 0.05$). NS, not significant; ND, not detected. Data are represented as mean ± SEM. *$p < 0.05$.

(Sadrzadeh et al., 2017). This is consistent with a prenatal programming contribution to obesity in women with PCOS.

Obesity is an outcome of a mismatch between energy intake and expenditure. There are inconsistent data regarding energy intake in women with PCOS, but the majority of studies found no differences in daily food and nutrient consumption in women with PCOS when compared with controls (Wright et al., 2004; Altieri et al., 2013). Wright et al. reported that women with PCOS with a normal BMI consumed a significantly lower number of calories (≥250 kcal/day) than BMI-matched controls, hypothesizing that this might be necessary to prevent weight gain in these women (Wright et al., 2004). Studies evaluating physical activity levels in women with and without PCOS are more consistent, reporting no difference in overall levels of physical activity (Álvarez-Blasco et al., 2011). A limited number of studies have looked at basal metabolic rate in women with PCOS, and most studies show no difference in PCOS when compared with weight-matched controls (Larsson et al., 2016). Collectively, these observations suggest that the defect is in adaptive EE.

We have previously assessed EE after feeding in women with PCOS using continuous indirect calorimetry (Robinson et al., 1992). These women show a reduction in peak PPT to 73.2% ± 6.9% of weight-matched controls (Robinson et al., 1992). Here we provide evidence from female sheep that suggests that this defect in EE can be prenatally programmed, by androgen in this case. The PCOS-sheep had an identical reduction in peak PPT (72.1% ± 7.9% of weigh-matched controls). This suggests that the high prevalence of obesity in women with PCOS may be related to altered adaptive thermogenesis that is not a consequence of obesity. There are a lot of discrepancies regarding the potential role of decreased PPT in obesity, mainly due to differences in patient selection and methodologies (Granata and Brandon, 2002). However, in women with PCOS, normalizing PPT, in the absence of increased energy intake, would be expected to promote weight loss to enhance health and well-being.

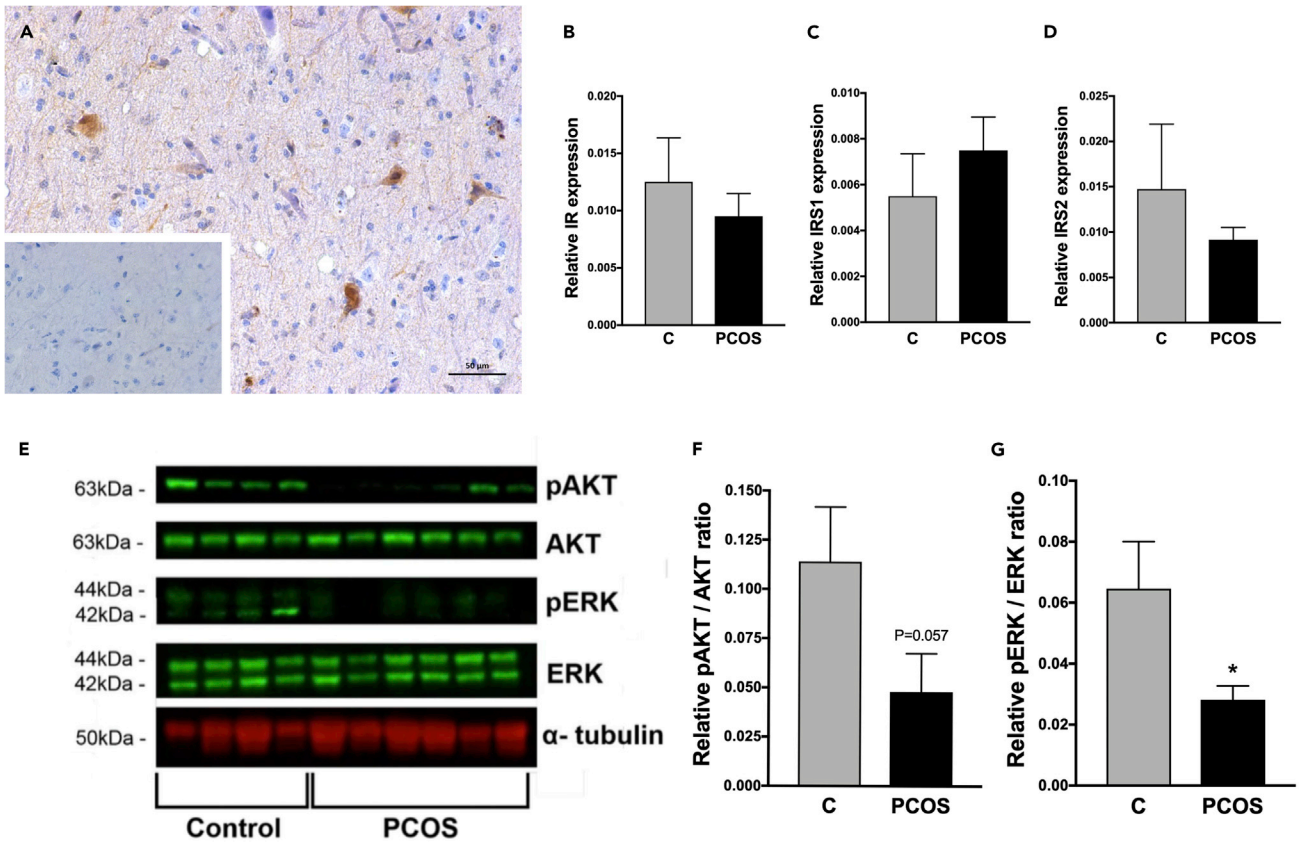

Figure 5. Central Insulin Signaling

(A–D) (A) Immunohistochemistry for pERK (brown) in the hypothalamus of C-sheep. Inset is negative control serial section. Relative mean gene expression ± SEM for (B) *INSR* (IR), (C) *IRS1*, and (D) *IRS2* in the frontal cortex of C-sheep and PCOS sheep.

(E) Representative western blot of AKT, phospho-AKT (pAKT), ERK, and phospho-ERK (pERK) in the frontal cortex of C-sheep and PCOS-sheep with α-tubulin as a loading control. The size representation in kDa, determined by a molecular weight marker ladder, is shown to the left. Sheep were sacrificed 15 min after an intravenous glucose bolus.

(F) Quantification of pAKT to ATK ratio in the frontal cortex in C-sheep and PCOS-sheep.

(G) Quantification of pERK to ERK ratio in the frontal cortex in C-sheep and PCOS-sheep. Scale bar, 50 μm. Data are represented as mean ± SEM. *$p < 0.05$.

To normalize PPT in women with PCOS it is necessary to interrogate the molecular mechanisms of reduced PPT. As rodents, with a small size and correspondingly high body surface area, have a large capacity for thermogenesis, as a consequence of brown adipose tissue (BAT) (Reitman, 2018), they are not ideal to study PPT in adult humans who do not have the same proportion of BAT. BAT is present in newborn lambs, whereas it cannot be routinely detected in adult sheep. In sheep like women there may be features of BAT, such as UCP expression, in "white" adipose tissue (WAT), but any changes in function are changes in the function of WAT rather than classical BAT. In addition, there are challenges recapitulating the entire phenotype of women with PCOS using rodent models (McNeilly and Duncan, 2013). The ovine model of PCOS, as a consequence of prenatal androgenization (Padmanabhan and Veiga-Lopez, 2013, Connolly et al., 2014; Hogg et al., 2012; Birch et al., 2003), provides a clinically realistic model of PCOS in a large animal with hormonal, ovarian, and metabolic phenotypes equivalent to women with PCOS. Importantly this model has the same obesity-independent deficit in PPT as seen in women with PCOS.

Thermogenesis is a consequence of increased heat generation by metabolic tissues independent of blood flow (Clarke et al., 2012). Effector tissues, such as fat, muscle, and liver, shape the thermogenic response by increasing heat generation. The defect in PPT seen in the PCOS-sheep is associated with a reduction in the expression of uncoupling proteins in adipose tissue. UCP1 is the master effector of thermogenesis in adipose tissue. Mice lacking UCP1 become obese when consuming normal diets (Feldmann et al., 2009). Rodents fed on a highly palatable diet voluntarily overfeed but have an ability to dissipate extra energy

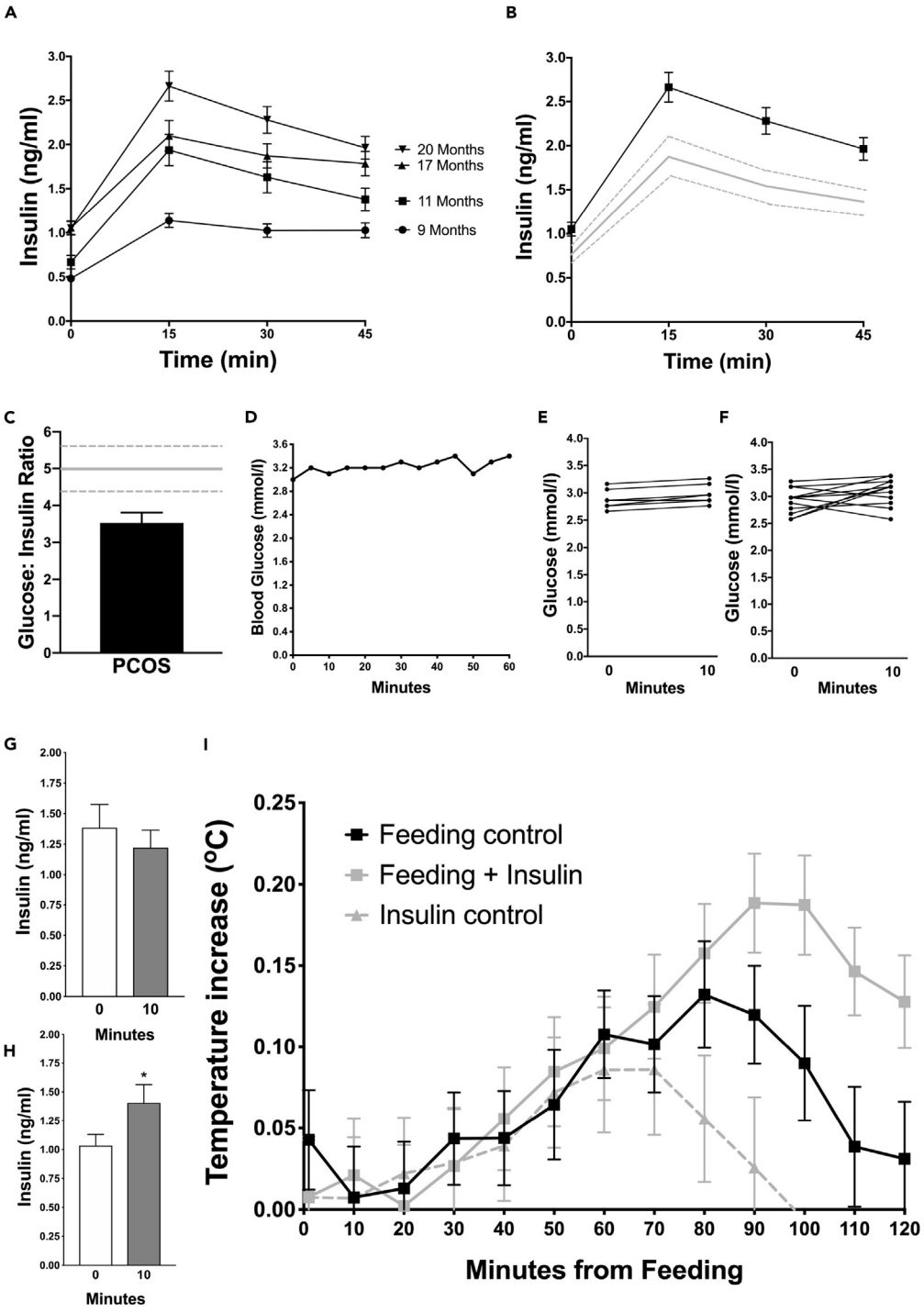

Figure 6. Intranasal Insulin Administration

(A) Assessment of plasma insulin concentrations before and up to 45 min after intravenous (i.v.) GTT in the second cohort of PCOS-sheep (n = 12) at 9, 11, 17, and 20 months of age.

(B) Plasma insulin concentrations after i.v. GTT at 20 months of age (black) showing the mean ± SEM of historical age-matched C-sheep (gray).

(C) The fasting glucose to insulin ratio in these PCOS-sheep with the mean ± SEM of historical age-matched C-sheep (gray).

(D–H) (D) The effect of 10 IU intranasal administration over 60 min of plasma glucose concentration in a single PCOS-sheep. The effect of 10 IU insulin 10 min after administration on plasma glucose in PCOS-sheep (n = 12) in the absence (E)

Figure 6. *Continued*
or presence (F) of feeding. The effect of 10 IU insulin 10 min after administration on plasma insulin in PCOS-sheep (n = 12) in the absence (G) or presence (H) of feeding.
(I) Temperature increase in PCOS-sheep at 20 months of age as a function of time from feeding (black), after feeding with 10 IU intranasal insulin (gray) and after 10 IU intranasal insulin without feeding (gray dashed line). Data are represented as mean ± SEM. *$p < 0.05$.

as heat with a significant increase in UCP1, both at mRNA and protein levels, in BAT (Falcou et al., 1985). Genetically fat sheep have reduced PPT when compared with lean animals, and this is likely to be a consequence of decreased UCP1 expression in retroperitoneal adipose tissue (Henry et al., 2015). Indeed, in human studies, UCP1 polymorphisms are related to decreased PPT (Nagai et al., 2003). The subpopulation of control sheep that were obese did not show a UCP expression like the PCOS-sheep highlighting further the prenatally programmed alterations in adult adipose tissue function.

Although the role of UCP1 in adaptive thermogenesis is well established, the precise function of UCP2 and UCP3 in cells remains unknown. As UCP2 and UCP3 have 60% sequence identity with UCP1 and 70% similarity with each other it is likely that they have similar biochemical functions (Esteves and Brand, 2005). Rodents overexpressing UCP2/UCP3 have decreased adiposity and are protected from diet-induced obesity (Horvath et al., 2003) although, unlike UCP1, UCP2/UCP3 may have a role in free fatty acid metabolism (Bezaire et al., 2005). A study in a dehydroepiandrosterone-induced rat model of PCOS demonstrated that PCOS-like rats have significantly reduced BAT activity with decreased UCP1 and lower thermogenic capacity (Yuan et al., 2016). However, UCP transcript abundance might not parallel protein expression and activity and there may be other explanations for the reduction in PPT in PCOS-sheep. Overall, though, it seems that reduced thermogenesis in the PCOS-sheep is a consequence of adipose tissue dysfunction.

There are several potential regulatory mechanisms driving the thermogenic response, but it is clear that the sympathetic nervous system has a major role in the overall regulation of PPT (Wijers et al., 2009). BAT thermogenesis is controlled by the sympathetic nervous system, where localized release and action of NA activates UCP1 (Tseng et al., 2010). Depletion of the adrenoceptors ADBR1, ADBR2, and ADBR3 in thermogenic adipose tissue results in an obese phenotype and decreased UCP1 expression (Lowell et al., 1993). Feeding is associated with sympathetic activation and increased sympathetic nerve firing, and this effect is regional as there is no increased NA spill to the heart or associated cardiovascular effects (Cox et al., 1995). This is correlated closely with heat production (Schwartz et al., 1987).

An adrenaline infusion increases PPT and peripheral oxygen consumption, which is reduced by β-blockade (Astrup et al., 1989). Women with diminished PPT have a normal thermic response to adrenaline suggesting that a reduction in sympathetic activity rather than sensitivity to adrenaline is involved in impaired PPT (Forbes et al., 2009). Starvation reduces the central sympathetic drive for thermogenesis (Wijers et al., 2009), and genetically obese rodents have lower sympathetic activity in BAT (Knehans and Romsos, 1982). To our knowledge there have been no studies looking at NA concentrations in the adipose tissue of women with PCOS but there is evidence for decreased adrenergic responses in adipose tissue from women with PCOS (Faulds et al., 2003). Overall this suggests that reduced sympathetic nervous system signaling in adipose tissue may be responsible for the reduced PPT.

IR and compensatory hyperinsulinemia are key factors contributing to the pathophysiology of PCOS (Diamanti-Kandarakis and Dunaif, 2012). It is estimated that as many as 50%–70% women with PCOS are insulin resistant, independent of BMI (DeUgarte et al., 2005; Stepto et al., 2013). On average, insulin sensitivity is decreased by 35%–40% in patients with PCOS when compared with matched controls (Diamanti-Kandarakis and Dunaif, 2012). The reduction in PPT in women with PCOS correlates with IR (Robinson et al., 1992), and this is also the case in the PCOS-sheep. This link between insulin sensitivity and reduced PPT has also been shown by others, although the mechanisms are still not fully understood (Ravussin et al., 1985; Camastra et al., 1999). However, peripheral IR has been shown to be associated with reduced insulin sensitivity in the central nervous system (CNS) (Benedict et al., 2011).

Insulin enters the CNS through the blood-brain barrier, and although the details of this process are unknown, it is thought to be through a receptor-mediated mechanism (Plum et al., 2005). Insulin receptors are widespread in the brain with high populations found in the cerebellum, cerebral cortex, hippocampus, hypothalamus, and the olfactory bulb (Bruning, 2000). Previous studies have demonstrated the critical role

of insulin signaling in response to food (Guthoff et al., 2010) and weight regulation with increasing insulin causing weight loss and inhibition of signaling causing weight gain (Plum et al., 2005). Reduced insulin signaling in the brain, in the presence of increased plasma insulin, has been identified in obese states highlighting a role of central insulin signaling in the pathophysiology of obesity (Kern et al., 2006). One thing that we were not able to investigate was transport of insulin into the CNS. It remains plausible that part of the reduced central insulin signaling relates to insulin transport as well as insulin action.

There is a sympathoexcitatory response to hyperinsulinemic clamp (Ward et al., 2011). Direct injections of insulin into the preoptic area of the mouse hypothalamus activate BAT thermogenesis and stimulate increase in core body temperature in a dose-dependent manner (Sanchez-Alavez et al., 2010), through neural mechanisms. In addition, the thermogenic activity in mouse BAT declines with insulin deficiency (Shibata et al., 1987). Direct administration of leptin into the brain also stimulates peripheral thermogenesis in large animal models through increased sympathetic nerve activity (Henry et al., 2008). We showed that insulin signaling in the brain of PCOS-sheep is reduced in the presence of the insulin receptor pathway. This is consistent with central insulin signaling having a key role in the regulation of PPT.

Nasal administration of proteins allows them to travel directly to the brain along the olfactory nerve and perivascular channels and is a novel strategy to facilitate central delivery and action (Meredith et al., 2015). In humans INI administration increases cerebrospinal fluid insulin concentrations within 60 min without adversely affecting blood insulin or glucose concentrations (Craft et al., 2012). In healthy men, INI did not change resting metabolism but increased PPT by 17% (Benedict et al., 2011). In Alzheimer disease there is reduced central insulin activity, and INI improved memory and functional ability without peripheral insulin effects (Craft et al., 2012). In pilot studies INI over 8 weeks reduced body fat in normal men (Hallschmid et al., 2004). This reduction was not seen in normal women (Hallschmid et al., 2004). However, this has not been examined in women with PCOS who, like men, are more insulin resistant, are exposed to increased androgens during development and adult life, and have more android fat distribution.

INI administration in humans is safe and has been assessed in Alzheimer disease (Craft et al., 2012), other neurological conditions, and diabetes mellitus (Fourlanos et al., 2011). There were no serious adverse events reported due to INI administration. In some articles, there were reports of nose soreness, nose bleeding, mild rhinitis, nasal dripping, and sneezing due to nasal administration. The doses of INI ranged from 20 to 160 IU in each single administration, with the highest dose in a single day totaling 420 IU (Ott et al., 2015). In our studies, to ensure safety, we opted to test a small dose of insulin and showed an effect at 10 IU. The administration of INI in sheep, like in humans, is well tolerated and safe.

INI has been used to investigate food intake in humans. Benedict et al. administered INI to normal-weight subjects before presenting an *ad libitum* breakfast buffet, to determine a possible difference in food intake between sexes (Benedict et al., 2011). Intranasal administration reduced the free-choice intake of carbohydrates. Food intake was reduced in men but not women, suggesting that men may be more sensitive to the anorexigenic effects of increased central insulin action. Men who had been administered INI exhibited a significant decrease in total calorie intake (Jauch-Chara et al., 2012). Food-related neuronal activity monitoring showed that INI increased the cerebral processing of food images in lean subjects, but there was no effect in obese subjects, suggesting a degree of central IR associated with obesity (Guthoff et al., 2011). INI is a safe therapeutic strategy to raise central nervous system insulin concentrations and action.

We suggest that women with PCOS may be prenatally programmed to have altered adaptive EE, manifest by a defect in PPT, which predisposes to obesity. INI taken with food will enhance the deficient central effects of this hormone and normalize the thermogenic response in effector tissues. In addition, INI alone without feeding also increased thermogenesis. INI may also have the added benefit of reducing food intake giving dual benefits in weight loss strategies. This suggests the utility of a pilot study investigating INI on PPT in women with PCOS. INI administration with food has the potential to be a convenient, accessible, and safe therapeutic strategy to normalize PPT and facilitate weight loss in women with PCOS.

Limitations of the Study

Although we used a clinically realistic large animal model, which showed the same defect in PPT as women with PCOS, further research in women is required to determine if the mechanistic and therapeutic elements discovered here translate into women with PCOS. We feel that this animal model used is the most suited to carrying out

this work. However, working with large animals with a long lead-time to adulthood gives particular experimental challenges with regard to molecular tools and replicates. We inferred biological activity in fat by looking at transcript abundance, and further research looking at detailed adipose tissue mitochondrial function *in vitro* would enhance the findings. In the therapeutic study we focused on PCOS-sheep, and doubling the size of the study to include contemporaneous randomized controls would have been a robust strategy, if additional funding was available. Similarly, additional animals where we were able to examine insulin signaling in the brain after nasal administration, rather than just systemic glucose administration, would have given valuable information.

Resource Availability

Lead Contact

The corresponding author, Professor W. Colin Duncan (w.c.duncan@ed.ac.uk).

Materials Availability

Requests for further information or materials should be directed to the lead contact.

Data and Code Availability

Requests for biological datasets should be directed to the lead contact.

METHODS

All methods can be found in the accompanying Transparent Methods supplemental file.

SUPPLEMENTAL INFORMATION

Supplemental Information can be found online at https://doi.org/10.1016/j.isci.2020.101164.

ACKNOWLEDGMENTS

The authors wish to acknowledge Joan Docherty, John Hogg, Marjorie Thomson, Peter Tennant, and James Nixon and the staff at the Marshall Building, University of Edinburgh, for their excellent animal husbandry. Dr Kirsten Hogg, Dr Fiona Connolly, Dr Junko Nio-Kobayashi, Dr Avi Lerner, and Lyndsey Boswell helped with tissue collection.

Funding: This work was funded by Medical Research Council (MRC) project grants (G0500717; G0801807; G0802782) and supported by the MRC Center for Reproductive Health (MR/N022556/1).

AUTHOR CONTRIBUTIONS

Conceptualization, W.C.D., S.F., K.S., and M.T.R.; Methodology, W.C.D., L.M.N., and M.T.R.; Formal Analysis, W.C.D., L.M.N., K.S., and F.H.; Investigation, W.C.D., L.M.N., M.T.R., K.S., F.N., and C.A.; Writing – Original Draft, W.C.D., L.M.N., C.A., F.N., and K.S.; Writing – Reviewing and Editing, W.C.D., S.F., M.T.R., and K.S.; Supervision, W.C.D., M.T.R., and S.F.; Funding Acquisition, W.C.D., M.T.R., and S.F.

DECLARATIONS OF INTERESTS

The authors declare no competing interests.

Received: January 2, 2020
Revised: April 8, 2020
Accepted: May 11, 2020
Published: June 26, 2020

REFERENCES

Abbott, D.H., Nicol, L.E., Levine, J.E., Xu, N., Goodzari, M.O., and Dumesic, D.A. (2013). Nonhuman primate models of polycystic ovary syndrome. Mol. Cell Endocrinol. *373*, 21–28.

Altieri, P., Cavazza, C., Pasqui, F., Morselli, A.M., Gambineri, A., and Pasquali, R. (2013). Dietary habits and their relationship with hormones and metabolism in overweight and obese women with polycystic ovary syndrome. Clin. Endocrinol. *78*, 52–59.

Álvarez-Blasco, F., Luque-Ramírez, M., and Escobar-Morreale, H.F. (2011). Diet composition and physical activity in overweight and obese premenopausal women with or without polycystic ovary syndrome. Gynecol. Endocrinol. *27*, 978–981.

Astrup, A., Simonsen, L., Bülow, J., Madsen, J., and Christensen, N.J. (1989). Epinephrine

mediates facultative carbohydrate-induced thermogenesis in human skeletal muscle. Am. J. Physiol. *257*, E340–E345.

Barnes, R.B., Rosenfield, R.L., Ehrmann, D.A., Cara, J.F., Cuttler, L., Levitsky, L.L., and Rosenthal, I.M. (1994). Ovarian hyperandrogenism as a result of congenital adrenal virilising disorders: evidence for prenatal masculinisation of neuroendocrine function in women. J. Clin. Endocrinol. Metab. *79*, 1328–1333.

Benedict, C., Brede, S., Schiöth, H.B., Lehnert, H., Schultes, B., and Hallschmid, M. (2011). Intranasal insulin enhances postprandial thermogenesis and lowers postprandial serum insulin levels in healthy men. Diabetes *60*, 114–118.

Bezaire, V., Spriet, L.L., Campbell, S., Sabet, N., Gerrits, M., Bonen, A., and Harper, M.E. (2005). Constitutive UCP3 overexpression at physiological levels increases mouse skeletal muscle capacity for fatty acid transport and oxidation. FASEB J. *19*, 977–979.

Birch, A., Padmanabhan, V., Foster, D.L., Unsworth, W.P., and Robinson, J.E. (2003). Prenatal programming of reproductive neuroendocrine function: fetal androgen exposure produces progressive disruption of reproductive cycles in sheep. Endocrinology *144*, 1426–1434.

Bruning, J. (2000). Role of brain insulin receptor in control of body weight and reproduction. Science *289*, 2122–2125.

Camastra, S., Bonora, E., Del Prato, S., Rett, K., Weck, M., and Ferrannini, E. (1999). Effect of obesity and insulin resistance on resting and glucose-induced thermogenesis in man. EGIR (European Group for the Study of Insulin Resistance). Int. J. Obes. Relat. Metab. Disord. *23*, 1307–1313.

Ching, H.L., Burke, V., and Stuckey, B.G. (2007). Quality of life and psychological morbidity in women with polycystic ovary syndrome: body mass index, age and the provision of patient information are significant modifiers. Clin. Endocrinol. *66*, 373–379.

Clarke, S.D., Lee, K., Andrews, Z.B., Bischof, R., Fahri, F., Evans, R.G., Clarke, I.J., and Henry, B.A. (2012). Postprandial heat production in skeletal muscle is associated with altered mitochondrial function and altered futile calcium cycling. Am. J. Physiol. Regul. Integr. Comp. Physiol. *303*, R1071–R1079.

Connolly, F., Rae, M.T., Butler, M., Kibanov, A.L., Sboros, V., McNeilly, A.S., and Duncan, W.C. (2014). The local effects of ovarian diathermy in an ovine model of polycystic ovary syndrome. PLoS One *9*, e111280.

Cox, H.S., Kaye, D.M., Thompson, J.M., Turner, A.G., Jennings, G.L., Itsiopoulos, C., and Esler, M.D. (1995). Regional sympathetic nervous activation after a large meal in humans. Clin. Sci. *89*, 145–154.

Craft, S., Baker, L.D., Montine, T.J., Minoshima, S., Watson, G.S., Claxton, A., Arbuckle, M., Callaghan, M., Tsai, E., Plymate, S.R., et al. (2012). Intranasal insulin therapy for Alzheimer disease and amnestic mild cognitive impairment: a pilot clinical trial. Arch. Neurol. *69*, 29–38.

DeUgarte, C.M., Bartolucci, A.A., and Azziz, R. (2005). Prevalence of insulin resistance in the polycystic ovary syndrome using the homeostasis model assessment. Fertil. Steril *83*, 1454–1460.

Diamanti-Kandarakis, E., and Dunaif, A. (2012). Insulin resistance and the polycystic ovary syndrome revisited: an update on mechanisms and implications. Endocr. Rev. *33*, 981–1030.

Esteves, T.C., and Brand, M.D. (2005). The reactions catalysed by the mitochondrial uncoupling proteins UCP2 and UCP3. Biochim. Biophys. Acta *1709*, 35–44.

Falcou, R., Bouillaud, F., Mory, G., Apfelbaum, M., and Ricquier, D. (1985). Increase of uncoupling protein and its mRNA in brown adipose tissue of rats fed on 'cafeteria diet'. Biochem. J. *231*, 241–244.

Faulds, G., Rydén, M., Ek, I., Wahrenberg, H., and Arner, P. (2003). Mechanisms behind lipolytic catecholamine resistance of subcutaneous fat cells in the polycystic ovarian syndrome. J. Clin. Endocrinol. Metab. *88*, 2269–2273.

Fauser, B.C., Tarlatzis, B.C., Reber, R.W., Legro, R.S., Balen, A.H., Lobo, R., Carmina, E., Chang, J., Yildiz, B.O., Laven, L.S., et al. (2012). Consensus on women's health aspects of polycystic ovary syndrome (PCOS): the Amsterdam ESHRE/ASRM-Sponsored 3rd PCOS Consensus Workshop Group. Fertil. Steril. *97*, 28–38.

Feldmann, H.M., Golozoubova, V., Cannon, B., and Nedergaard, J. (2009). UCP1 ablation induces obesity and abolishes diet-induced thermogenesis in mice exempt from thermal stress by living at thermoneutrality. Cell Metab. *9*, 203–209.

Forbes, S., Robinson, S., Parker, K.H., Macdonald, I.A., McCarthy, M.I., and Johnston, D.G. (2009). The thermic response to food is related to sensitivity to adrenaline in a group at risk for the development of type II diabetes. Eur. J. Clin. Nutr. *63*, 1360–1367.

Fourlanos, S., Perry, C., Gellert, S.A., Martinuzzi, E., Mallone, R., Butler, J., Colman, P.G., and Harrison, L.C. (2011). Evidence that nasal insulin induces immune tolerance to insulin in adults with autoimmune diabetes. Diabetes *60*, 1237–1245.

Gore, A.C., Chappell, V.A., Fenton, S.E., Flaws, J.A., Nadal, A., Prins, G.S., Toppari, J., and Zoeller, R.T. (2015). EDC-2: the endocrine society's second scientific statement on endocrine-disrupting chemicals. Endocr. Rev. *36*, E1–E150.

Granata, G.P., and Brandon, L.J. (2002). The thermic effect of food and obesity: discrepant results and methodological variations. Nutr. Rev. *60*, 223–233.

Guthoff, M., Grichisch, Y., Canova, C., Tschritter, O., Veit, R., Hallschmid, M., Häring, H.U., Preissl, H., Hennige, A.M., and Fritsche, A. (2010). Insulin modulates food-related activity in the central nervous system. J. Clin. Endocrinol. Metab. *95*, 748–755.

Guthoff, M., Stingl, K.T., Tschritter, O., Rogic, M., Heni, M., Dtingl, K., Hallschmid, M., Häring, H.-U., Fritsche, A., Preissl, H., et al. (2011). The insulin-mediated modulation of visually evoked magnetic fields is reduced in obese subjects. PLoS One *6*, e19482.

Hales, C.N., and Barker, D.J.P. (1992). Type 2 (non-insulin-dependent) diabetes mellitus: the thrifty phenotype hypothesis. Diabetologia *35*, 595–601.

Hallschmid, M., Benedict, C., Schultes, B., Fehm, H.L., Born, J., and Kern, W. (2004). Intranasal insulin reduces body fat in men but not in women. Diabetes *53*, 3024–3029.

Henry, B.A., Dunshea, F.R., Gould, M., and Clarke, I.J. (2008). Profiling postprandial thermogenesis in muscle and fat of sheep and the central effect of leptin administration. Endocrinology *149*, 2019–2026.

Henry, B.A., Loughnan, R., Hickford, J., Young, I.R., St John, J.C., and Clarke, I. (2015). Differences in mitochondrial DNA inheritance and function align with body conformation in genetically lean and fat sheep. J. Anim. Sci. *93*, 2083–2093.

Hogg, K., Wood, C., McNeilly, A.S., and Duncan, W.C. (2011). The in utero programming effect of increased maternal androgens and a direct fetal intervention on liver and metabolic function in adult sheep. PLoS One *6*, e24877.

Hogg, K., Young, J.M., Oliver, E.M., Souza, C.J., McNeilly, A.S., and Duncan, W.C. (2012). Enhanced thecal androgen production is prenatally programmed in an ovine model of polycystic ovary syndrome. Endocrinology *153*, 450–461.

Horvath, T.L., Diano, S., Miyamoto, S., Barry, S., Gatti, S., Alberati, D., Livak, F., Lombardi, A., Moreno, F., Goglia, F., et al. (2003). Uncoupling proteins-2 and 3 influence obesity and inflammation in transgenic mice. Int. J. Obes. Relat. Metab. Disord. *27*, 433–442.

Isganaitis, E. (2019). Developmental programming of body composition: update on evidence and mechanisms. Curr. Diab. Rep. *19*, 60.

Jason, J. (2011). Polycystic ovary syndrome in the United States: clinical visit rates, characteristics, and associated health care costs. Arch. Intern. Med. *171*, 1209–1211.

Jauch-Chara, K., Friedrich, A., Rezmer, M., Melchert, U.H., Scholand-Engler, H., Hallschmid, M., and Oltmanns, K.M. (2012). Intranasal insulin suppresses food intake via enhancement of brain energy levels in humans. Diabetes *61*, 2261–2268.

Kern, W., Benedict, C., Schultes, B., Plohr, F., Moser, A., Born, J., Fehm, H.L., and Hallschmid, M. (2006). Low cerebrospinal fluid insulin levels in obese humans. Diabetologia *49*, 2790–2792.

Knehans, A.W., and Romsos, D.R. (1982). Reduced norepinephrine turnover in brown adipose tissue of ob/ob mice. Am. J. Physiol. *242*, E253–E261.

Larsson, I., Hulthén, L., Landén, M., Pålsson, E., Janson, P., and Stener-Victorin, E. (2016). Dietary intake, resting energy expenditure, and eating

behavior in women with and without polycystic ovary syndrome. Clin. Nutr. *35*, 213–218.

Legro, R.S., Gnatuk, C.L., Kunselman, A.R., and Dunaif, A. (2005). Changes in glucose tolerance over time in women with polycystic ovary syndrome: a controlled study. J. Clin. Endocrinol. Metab. *90*, 3236–3242.

Lowell, B.B., S-Susulic, V., Hamann, A., Lawitts, J.A., Himms-Hagen, J., Boyer, B.B., Kozak, L.P., and Flier, J.S. (1993). Development of obesity in transgenic mice after genetic ablation of brown adipose tissue. Nature *366*, 740–742.

McNeilly, A.S., and Duncan, W.C. (2013). Rodent models of polycystic ovary syndrome. Mol. Cell. Endocrinol *373*, 2–7.

Meredith, M.E., Salameh, T.S., and Banks, W.A. (2015). Intranasal delivery of proteins and peptides in the treatment of neurodegenerative diseases. AAPS J. *17*, 780–787.

Nagai, N., Sakane, N., Ueno, L.M., Hamada, T., and Moritani, T. (2003). The -3826 A–>G variant of the uncoupling protein-1 gene diminishes postprandial thermogenesis after a high fat meal in healthy boys. J. Clin. Endocrinol. Metab. *88*, 5661–5667.

Ollila, M.M., Piltonen, T., Puukka, K., Ruokonen, A., Järvelin, M.R., Tapanainen, J.S., Franks, S., and Morin-Papunen, L. (2016). Weight gain and dyslipidemia in early adulthood associate with polycystic ovary syndrome: prospective cohort study. J. Clin. Endocrinol. Metab. *101*, 739–747.

Ott, V., Lehnert, H., Staub, J., Wönne, K., Born, J., and Hallschmid, M. (2015). Central nervous insulin administration does not potentiate the acute glucoregulatory impact of concurrent mild hyperinsulinemia. Diabetes *64*, 760–765.

Padmanabhan, V., and Veiga-Lopez, A. (2013). Sheep models of polycystic ovary syndrome phenotype. Mol. Cell. Endocrinol. *373*, 8–20.

Palomba, S., Falbo, A., Zullo, F., and Orio, F., Jr. (2009). Evidence-based and potential benefits of metformin in the polycystic ovary syndrome: a comprehensive review. Endocr. Rev. *30*, 1–50.

Plum, L., Schubert, M., and Brüning, J. (2005). The role of insulin receptor signaling in the brain. Trends Endocrinol. Metab. *16*, 59–65.

Rae, M., Grace, C., Hogg, K., Wilson, L.M., McHaffie, S.L., Ramaswamy, S., MacCallum, J., Connolly, F., McNeilly, A.S., and Duncan, C. (2013). The pancreas is altered by in utero androgen exposure: implications for clinical conditions such as polycystic ovary syndrome (PCOS). PLoS One *8*, e56263.

Ramaswamy, S., Grace, C., Mattei, A.A., Siemienowicz, K., Brownlee, W., MacCallum, J., McNeilly, A.S., Duncan, W.C., and Rae, M.T. (2016). Developmental programming of polycystic ovary syndrome (PCOS): prenatal androgens establish pancreatic islet α/β cell ratio and subsequent insulin secretion. Sci. Rep. *6*, 27408.

Ravelli, G.P., Stein, Z.A., and Susser, M.W. (1976). Obesity in young men after famine exposure in utero and early infancy. N. Engl. J. Med. *295*, 349–353.

Ravussin, E., Acheson, K.J., Vernet, O., Danforth, E., and Jéquier, E. (1985). Evidence that insulin resistance is responsible for the decreased thermic effect of glucose in human obesity. J. Clin. Invest. *76*, 1268–1273.

Reitman, M.L. (2018). Of mice and men - environmental temperature, body temperature, and treatment of obesity. FEBS Lett. *592*, 2098–2107.

Robinson, S., Chan, S.-P., Spacet, S., Anyaoku, V., Johnston, D.G., and Franks, S. (1992). Postprandial thermogenesis is reduced in polycystic ovary syndrome and is associated with increased insulin resistance. Clin. Endocrinol. *36*, 537–543.

Sadrzadeh, S., Hui, E.V.H., Schoonmade, L.J., Painter, R.C., and Lambalk, C.B. (2017). Birthweight and PCOS: systematic review and meta-analysis. Hum. Reprod. Open *2017*, hox010.

Sanchez-Alavez, M., Tabarean, I.V., Osborn, O., Mitsukawa, K., Schaefer, J., Dubins, J., Holmberg, K.H., Klein, I., Klaus, J., Gomez, L.F., et al. (2010). Insulin causes hyperthermia by direct inhibition of warm-sensitive neurons. Diabetes *59*, 43–50.

Schwartz, R.S., Jaeger, L.F., Silberstein, S., and Veith, R.C. (1987). Sympathetic nervous system activity and the thermic effect of feeding in man. Int. J. Obes. *11*, 141–149.

Shibata, H., Pérusse, F., and Bukowiecki, L.J. (1987). The role of insulin in nonshivering thermogenesis. Can. J. Physiol. Pharmacol. *65*, 152–158.

Sill, E.S., Perloe, M., Tucker, M.J., Kaplan, C.R., Genton, M.G., and Schattman, G.L. (2001). Diagnostic and treatment characteristics of polycystic ovary syndrome: descriptive measurements of patient perception and awareness from 657 confidential self-reports. BMC Womens Health *1*, 3.

Stepto, N.K., Cassar, S., Joham, A.E., Hutchison, S.K., Harrison, C.L., Goldstein, R.F., and Teede, H.J. (2013). Women with polycystic ovary syndrome have intrinsic insulin resistance on euglycaemic-hyperinsulaemic clamp. Hum. Reprod. *28*, 777–784.

Tseng, Y.-H., Cypess, A.M., and Kahn, C.R. (2010). Cellular bioenergetics as a target for obesity therapy. Nat. Rev. Drug Discov. *9*, 465–482.

Ward, K.R., Bardgett, J.F., Wolfgang, L., and Stocker, S.D. (2011). Sympathetic response to insulin is mediated by melanocortin 3/4 receptors in the hypothalamic paraventricular nucleus. Hypertension *57*, 435–441.

Wijers, S.L., Saris, W.H., and van Marken Lichtenbelt, W.D. (2009). Recent advances in adaptive thermogenesis: potential implications for the treatment of obesity. Obes. Rev. *10*, 218–226.

Wright, C.E., Zborowski, J.V., Talbott, E.O., McHugh-Pemu, K., and Youk, A. (2004). Dietary intake, physical activity, and obesity in women with polycystic ovary syndrome. Int. J. Obes. Relat. Metab. Disord. *28*, 1026–1032.

Yuan, X., Hu, T., Zhao, H., Huang, Y., Ye, R., Lin, J., Zhang, C., Zhang, H., Wei, G., Zhou, H., et al. (2016). Brown adipose tissue transplantation ameliorates polycystic ovary syndrome. Proc. Natl. Acad. Sci. U S A *113*, 2708–2713.

iScience, Volume *23*

Supplemental Information

Insights into Manipulating Postprandial Energy Expenditure to Manage Weight Gain in Polycystic Ovary Syndrome

Katarzyna Siemienowicz, Michael T. Rae, Fiona Howells, Chloe Anderson, Linda M. Nicol, Stephen Franks, and William C. Duncan

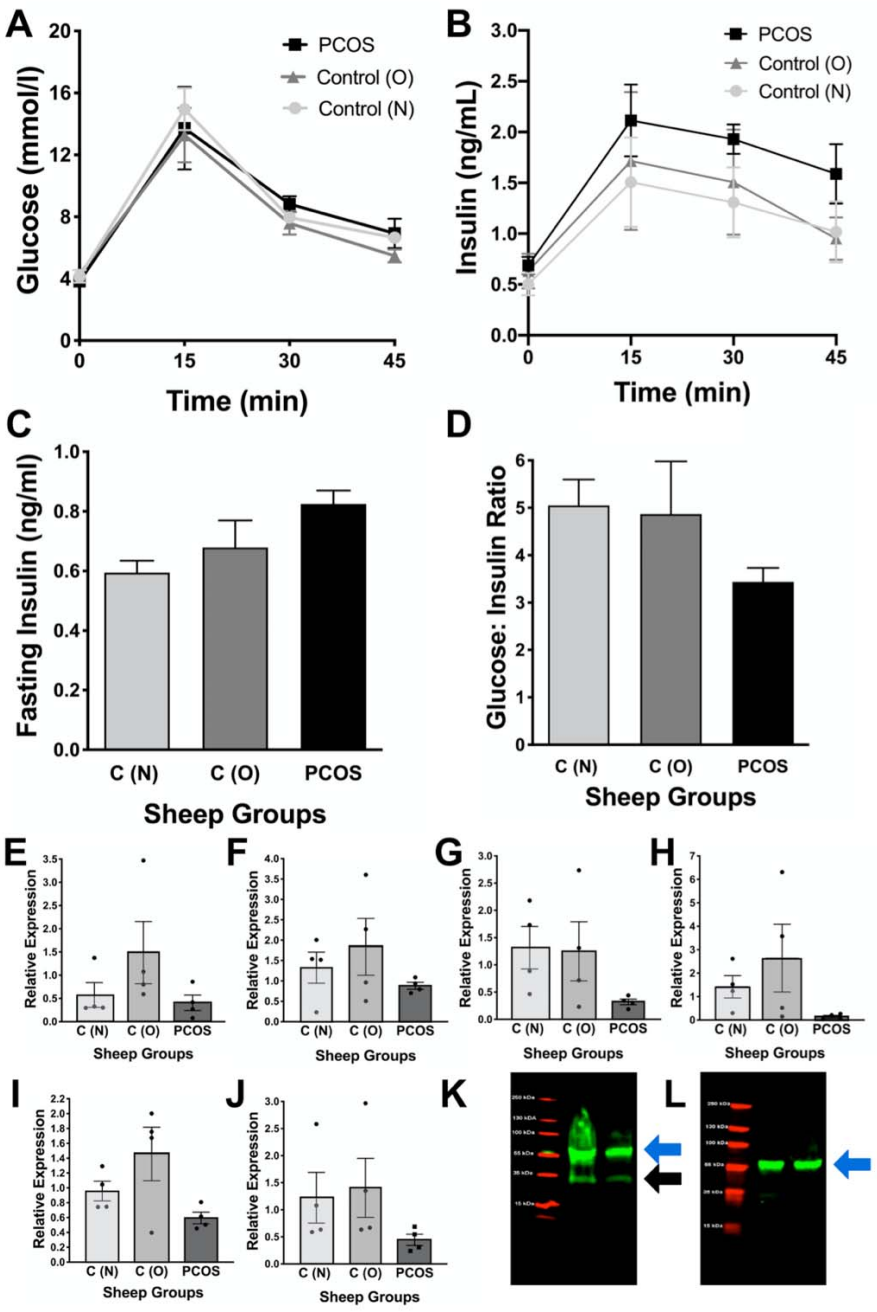

Figure S1. Related to Figures 2 and 3. Breakdown of the subset of sheep. Control normal sheep [C (N); n=4], control obese sheep [C (O); n=4] and PCOS-sheep [PCOS; n=4]. (**A**) Plasma glucose and (**B**) insulin in the 45 minutes after an IV GTT in C-sheep and PCOS-sheep at 24 months of age. **C**) Fasting insulin concentrations and (**D**) Fasting glucose to insulin ratio at 30 months of age. Relative expression of UCP1 in neck (**E**), back (**F**), visceral (**G**) and groin fat (**H**). Relative expression of UCP2 (**I**) and UCP3 (**J**) in back fat. (**K**) Western blot checking the specificity of the UCP3 antibody in sheep adipose tissue showing the UCP3 band at 34kDa (black arrow) as well as a non-specific band at 55kDa (blue arrow). (**L**) The same band is present when using normal goat serum in the negative controls highlighting that the differences between immunostained samples and negative controls is the specific UCP3 band. Data are represented as mean ±SEM.

Transparent Methods

All reagents and chemicals were obtained from Merc, former Sigma-Aldrich (Gillingham, UK), unless otherwise stated. Scottish Greyface ewes were housed in groups in spacious enclosures and fed hay *ad libitum*, supplemented with Excel Ewe Nuts (0.5-1.0kg/day; Carrs Billington, Lancashire, UK) and Crystalyx Extra High Energy Lick (Caltech Solway Mills, Cumbria, UK).

The ovine PCOS model

Ewes with a healthy body condition score (2.5-3) were synchronised with Chronogest (flugestone) sponges (Intervet UK Ltd, Buckinghamshire, UK) and Estrumate (cloprostenol) injection (Schering Plough Animal Health, Welwyn Garden City, UK) and mated with a Texel ram as described previously (Hogg et al., 2011). Pregnancy was suggested by lack of estrous and confirmed by ultrasound scanning. Pregnant ewes were treated twice weekly with IM testosterone propionate (100mg) in vegetable oil or vegetable oil control from day (D)62 to D102 of D147 pregnancy as described previously (Hogg et al., 2011, Rae et al., 2013). Lambs were weaned at 3 months. Female offspring were examined in this study. In the first cohort n=11 C-sheep and n=4 PCOS-sheep were studied and sacrificed at 30 months. In the second cohort n=12 PCOS-sheep were studied and sacrificed at 20 months. Fifteen minutes prior to sacrifice all sheep were given an IV bolus of glucose (500mg/ml in 20ml). Tissues of interest were fixed in Bouins solution for 24h, transferred to 70% ethanol and processed into paraffin wax and/or snap frozen and stored at -80^{o}C. We chose three sites for the collection of subcutaneous adipose tissue; the groin as this is commonly used as a collection site and the neck and intrascapular back fat as these are the sites where brown adipose tissue if it exists is more likely to be found.

Assessment of postprandial thermogenesis

Datalogger thermometers (Tethered SubCue; Canadian Analytical Technologies Inc, Calgary, Canada) were implanted into the interscapular adipose tissue under local anaesthetic with the download lead exteriorised. Animals recovered from the surgery for 10 days prior to assessment. PPT assessment was conducted in the non-breeding season to eliminate any bias secondary to differential ovarian function (e.g. differences in progesterone). After the use of a feeding schedule to entrain a morning feeding response, the ewes were studied on two separate days with identical nutritional input. Then the animals were kept in individual pens from 09.00h until 16.00h allowing them to sit or stand but excluding further movement. Temperature was recorded every minute before during and after timed feeding. The data from the two experiments were combined and the mean data used for analysis.

Intravenous glucose tolerance testing

Sheep were fasted overnight and a basal blood sample was taken and decanted into a heparinised tube for future plasma insulin assessment and tube containing sodium fluoride for blood glucose measurement. After an IV bolus of glucose (10g in 20ml saline) repeat blood samples were taken at 15, 30 and 45min. Tubes were centrifuged at 1200g for 15min at 4^{o}C and plasma collected and stored at -20^{o}C. Glucose was measured with an enzymatic-colourimetric assay kit (Alpha Laboratories Ltd, Eastleigh, UK) using a Cobas Fara analyser (Roche Diagnostics Ltd, UK). The assay sensitivity was 0.2mmol/l and the intra- and inter-assay CVs were <2% and <3% respectively. Insulin was measured using the ALPCO ovine Insulin Elisa kit (American Laboratory Products Company, Salem, USA) as per the

manufacturer's instructions. The assay sensitivity was 0.14ng/ml and the intra- and inter-assay CVs were <5% and <6% respectively.

Quantitative real-time polymerase chain reaction (RT-PCR)

RNA was extracted from adipose tissue with a combination of TRI Reagent with the RNeasy kit (Qiagen Ltd., West Sussex, UK). RNA was extracted from skeletal muscle using RNeasy Fibrous Tissue Mini Kit (Qiagen Ltd.). RNA was extracted from cerebral tissue using the RNeasy Mini Kit following the manufacturer's instructions. On-column DNase digestion was performed using RNase-Free DNase set (Qiagen Ltd.) and RNA concentration and purity was assessed using a NanoDrop One spectrometer (ThermoFisher Scientific, Loughborough, UK). Complementary DNA was synthesized using TaqMan RT reagents kit (Applied Biosystems, Warrington, UK) as described previously (Hogg et al., 2012). To select the most stable house-keeping genes the geNorm Reference Gene Selection Kit (Primerdesign Ltd., Southampton, UK) was used. For brain and muscle the housekeeping gene was *GAPDH*, for visceral fat a geometric mean of *RPS26* and *18S* and for subcutaneous fat the geometric mean of *ACTB* and *MDH1*.

Intron-spanning forward and reverse primers were designed using Primer3Plus online software (http://www.bioinformatics.nl/cgi-bin/primer3plus/primer3plus.cgi) from DNA sequences obtained at Ensembl Genome Browser (http://ensembl.org/index.html) and confirmed to be specific using the Basic Local Alignment Search Tool provided by the National Centre for Biotechnology Information. Primers (Table 1) were synthesised by Eurofins MWG (Ebersberg, Germany). Real time RT-PCR was performed on 384-well plate format (Applied Biosystems) with all samples run in duplicate and housekeeping control genes included in each run, as well as template, RNA and RT-negative controls, using the ABI 7900HT Fast Real Time PCR system (Applied Biosystems) as described previously (Hogg et al., 2012, Connolly et al., 2014). The transcript abundance of target gene relative to the housekeeping genes was quantified using the $\Delta\Delta$Ct method (Livak and Schmittgen, 2001).

Immunohistochemistry

Immunohistochemistry was performed as described previously (Connolly et al., 2013). After dewaxing and rehydrating sides were submerged in a citrate buffer (0.05M, pH 6) and pressure cooked for 5min before cooling and washing. Sections were immersed in 3% H_2O_2 for 10 minutes before endogenous biotin activity was blocked using an avidin/biotin kit (Vector Laboratories, Peterborough, UK). Slides were then incubated with blocking serum matching the host species of the antibody diluted in 5% bovine serum albumin (BSA). After optimisation experiments, the primary antibody diluted in blocking serum, or an equivalent concentration of non-specific matched immunoglobulins as negative control, was added overnight at 4^{o}C. After washing, the secondary antibody was applied for an hour diluted 1:500 in blocking serum and the slides were incubated with the ABC Elite complex (Vector Laboratories) for 1 hour before colourimetric visualisation using diamino-benzidine (Vector Laboratories). The reaction was stopped by washing in water, and slides were counterstained with haematoxylin, dehydrated and mounted.

The UCP1 antibody (polyclonal goat, M-17; sc-629; Santa Cruz Biotechnology Inc., Dallas, TX) and the UCP3 antibody (polyclonal goat, C-20; sc7756; Santa Cruz Biotechnology Inc.) were used at 1:100 dilution with a rabbit anti-goat biotinylated (BA-5000; Vector Laboratories) secondary antibody. The anti-phosphoERK antibody (polyclonal rabbit, (Phospho-p44/42 MAPK Erk1/2; 20G11; Cell Signalling Technology, London, UK) was used at

1:400 dilution and negative control was primary antibody pre-incubated with blocking peptide (Phospho-p44/42 MAPK Erk1/2, Blocking Peptide #1150; Cell Signalling Technology) and the secondary antibody was biotinylated goat anti-rabbit IgG (Vector Laboratories Ltd).

Gene	Forward Sequence	Reverse Sequence	Size (bp)
GAPDH	GGCGTGAACCACGAGAAGTATAA	AAGCAGGGATGATGTTCTGG	229
ACTB	ATCGAGGACAGGATGCAGAA	CCAATCCACACGGAGTACTTG	101
MDH1	TTATCTCCGATGGCAACTCC	GGGAGACCTTCAACAACTTTCC	100
RPS26	CAAGGTAGTCAGGAATCGCTCT	TTACATGGGCTTTGGTGGAG	106
18S	CAACTTTCGATGGTAGTCG	CCTTCCTTGGATGTGGTA	110
RYR1	GGACCTCATCGGCTACTTTG	GACATTTAGGCGGTCAATGC	151
ATP2A1	GACAGGGTAGATGGGGACCT	GTCCAAGGAGGAGTCATTGC	171
ATP2A2	GGTGCTCCTGAAGGTGTCAT	CAGTGGGTTGTCATGAGTGG	168
UCP1	AGAGCCATCTCCACGGTCCCA	CCAAAGCCCCGTCAAG	92
UCP2	AAGGCCCACCTAATGACAGA	CCCAGGGCAGAGTTCATGT	128
UCP3	AGATGAGCTTCGCCTCCAT	TGAAAGCGGATCTTCACCAC	172
ADRB1	CTTCTTCCTGGCCAACGTG	GGGTTGAAGGCCGAGTTG	105
ADRB2	CATGCCCAAAACGTCAGTC	TCTTGAGGGCTTTGTGTTCC	100
ADRB3	GCACCCAATACTGCCAACG	GTTGGTCATGGTCTGGAGTCT	159
INSR	CACCATCACTCAGGGGAAAC	CAGGAGGTCTCGGAAGTCAG	247
IRS1	ATCATCAACCCCATCAGACG	GAGTTTGCCACTACCGCTCT	240
IRS2	CCCGCGCCGGTGGCCCGCATCA	AGCAACACGCCCGAGTCCATC	263

Table 1. PCR primers
Forward and reverse primer sequences and product sizes for genes analysed in adipose and cerebral tissues.

Western blotting

Tissues (30-50mg) were homogenised in lysis buffer (150mM NaCl, 10mM Tris pH 7.4, 1mM EDTA, 1mM EGTA, 1% TrixonX-100, 0.5% NP-40, 0.5mM phenylmethyl sulfonyl fluoride, supplemented with 1 Complete mini tablet and 1 PhosSTOP tablet (Roche, West Sussex, UK) per 10 ml buffer.) Samples were pre-cleared by incubating with Protein G agarose beads (Cell Signalling Technology) for 1 hour at 4°C. Protein concentration was quantified using a Bio-Rad DC protein assay (Bio-Rad Laboratories Ltd, UK) kit following manufacturer's instructions. Samples (25µg) were diluted in Laemmli loading buffer (62.5 mM Tris, pH 6.8, 2% SDS, 1% β-mercaptoethanol, 10% Glycerol, 0.01% Bromophenol Blue), denatured by heating to 95°C for 5 min and loaded on 15 well 12% mini- PROTEAN TGX precast gels (Bio-Rad Laboratories Ltd, Watford, UK) alongside pre-stained full-range molecular weight markers (GE Healthcare, Buckinghamshire, UK). Proteins were then transferred onto Immobilon-FL polyvinylidene difluoride (PVDF) membrane (Merck Millipore Ltd, Cork, Ireland) using a wet tank transfer system.

Membranes were dried, rinsed and blocked for 1 hour at room temperature in Odyssey Blocking Buffer (PBS; LI-COR Biotechnology-UK Ltd, Cambridge) and then probed with the primary antibodies raised against phospho-ERK (Phospho-p44/42 MAPK (Erk1/2)

(Thr202/Tyr204) Antibody #9101 Cell Signalling Technology) or phospho-AKT (Phospho-Akt (Ser473) (D9E) XP Rabbit mAb #4060, Cell Signalling Technology) at 1:1000 in blocking buffer. Mouse anti-α -Tubulin (Sigma Aldrich, UK) at 1:3000 was used as a control for protein loading. For UCP3 western blots the primary antibody (polyclonal goat anti-human) was used at a concentration of 1:200 with the negative control 1:200 of 10% normal goat serum. The membrane was incubated in the primary antibody solution overnight at 4°C with gentle agitation. After washing the membrane was incubated in secondary antibody solution (1:10000 IRDye 800CW Donkey-anti-Rabbit, IgG + 1:10,000 IRDye 680RD Donkey anti-Mouse IgG; LI-COR Biotechnology, Cambridge, UK) or Donkey anti-Goat IRDye 800 at 1:10000 dilution, in blocking buffer, washed and visualised on the Odyssey Fc Imaging System (LI-COR Biotechnology). After visualisation, antibodies were stripped from the membranes using stripping buffer (25mM glycine pH 2, 1% SDS) and re-labelled with primary antibody for either total-ERK (p44/42 MAPK (Erk1/2) Antibody #9102; Cell Signalling Technology) or total-AKT (Akt Antibody #9272, Cell Signalling Technology). Protein was quantified using Image Studio Lite v5.2 (LI-COR Biotechnology) and the ratio of phosphorylated protein: total protein calculated.

Noradrenaline ELISA

A representative sample of adipose tissue was cut on dry ice and homogenised in homogenisation buffer (HCl 0.01N; EDTA 1mM; sodium metabisulfite ($Na_2S_2O_5$) 4mM) using TissueLyser (Qiagen Ltd.) at 25Hz for 4 min. The protein concentration of the homogenate supernatant was quantified by the Bradford assay. Noradrenaline concentrations were measured using Noradrenaline Research ELISA (ImmunSmol, BA E-5200, Pessac, France) as per the manufacturer's instructions. All samples were assayed in duplicate and results were corrected by the total protein content in the sample. The assay sensitivity was 0.1ng/ml and intra- and inter-assay CVs were <8.4% and <6.9% respectively.

Intranasal insulin

For the second cohort of PCOS-sheep small implantable temperature data loggers (DST Mini-T; AnimaLab, Poznan, Poland) were implanted into the interscapular adipose tissue under local anaesthetic. Animals recovered from the surgery for 10 days prior to assessment. After the use of a feeding schedule to entrain a morning feeding response the ewes were studied on 9 separate occasions in individual pens from 09.00h until 16.00h. Temperature was recorded every minute before during and after timed feeding. Three interventions were conducted in triplicate. The data from the three replications were combined and the mean data used for analysis. The three interventions assessed were: eating alone, eating with intranasal insulin (10IU; Hypurin bovine insulin; Intervet UK Ltd.; diluted in saline to 0.5ml) administered through LMA MAD Nasal Intranasal Mucosal Atomisation Device (Teleflex, Athlone, Ireland) to the left nostril, or intranasal insulin alone administered as above. In pilot experiments blood samples were measured every 5 minutes for glucose assessment. In the first run of each experiment blood was taken before and 10 minutes after nasal insulin administration for glucose and insulin assessment.

Statistics

Statistical analysis was performed with GraphPad Prism version 6.0 (GraphPad Software Inc., San Diego, CA). For comparing means of two groups with equal variances an unpaired, two-tailed, Student's t-test was used. Log transformation was used to allow for parametric analysis when necessary. For more than two comparisons ANOVA was used with Bonferroni

pairwise comparisons. Results are presented as Mean ±SEM and a P-value of <0.05 was considered statistically significant. Area under the curve (AUC) was calculated using the trapezoidal method. Correlation was assessed by calculation of the Pearson R co-efficient and a line of best fit was incorporated for statistically significant correlations. The maximal postprandial temperature response was calculated as the average time from feeding to the first reading of the peak temperature per sheep.

Study approval

These studies were conducted after institutional ethics review and UK Home Office approval (PPL60/4401). All experiments complied with the relevant regulatory standards.

Supplemental References

Connolly, F., Rae, M.T., Bittner, L., Hogg, K., McNeilly, A.S., Duncan, W.C. (2013) Excess androgens in utero alters fetal testis development. Endocrinology 154, 1921-1933.

Connolly, F., Rae, M.T., Butler, M., Kibanov, A.L., Sboros, V., McNeilly, A.S., Duncan, W.C. (2014) The local effects of ovarian diathermy in an ovine model of polycystic ovary syndrome. PLoS One 9, e111280.

Hogg, K., Wood, C., McNeilly, A.S., Duncan, W.C. (2011) The in utero programming effect of increased maternal androgens and a direct fetal intervention on liver and metabolic function in adult sheep. PLoS One 6, e24877.

Hogg, K., Young, J.M., Oliver, E.M., Souza, C.J., McNeilly, A.S., Duncan, W.C. (2012) Enhanced thecal androgen production is prenatally programmed in an ovine model of polycystic ovary syndrome. Endocrinology 153, 450-461.

Livak, K.J., Schmittgen, T.D. (2001) Analysis of relative gene expression data using real-time quantitative PCR and the 2-DDCT method. Methods 25, 402-408.

Rae, M., Grace, C., Hogg, K., Wilson, L.M., McHaffie, S.L., Ramaswamy, S., MacCallum, J., Connolly, F., McNeilly, A.S., Duncan, C. (2013) The pancreas is altered by in utero androgen exposure: implications for clinical conditions such as polycystic ovary syndrome (PCOS). PLoS One 8, e56263.